

AFGL-TR-88-0161

DTIC FILE COPY

Absolute Absorption Cross Section Measurements of
Ozone and the Temperature Dependence at Four
Reference Wavelengths Leading to Renormalization
of the Cross Section Between 240 and 350 nm

W. H. Parkinson
K. Yoshino
D. E. Freeman

Smithsonian Institution
Astrophysical Observatory
Cambridge, MA 02138

March 1988

Final Report
24 July 1985-31 December 1987

APPROVED FOR PUBLIC RELEASE; DISTRIBUTION UNLIMITED

AIR FORCE GEOPHYSICS LABORATORY
AIR FORCE SYSTEMS COMMAND
UNITED STATES AIR FORCE
HANSCOM AIR FORCE BASE, MASSACHUSETTS 01731-5000

DTIC
ELECTE
SEP 27 1988
S H D

88 9 27 13 6

AD-A199 737

"This technical report has been reviewed and is approved for publication"

Gail P. Anderson
(Signature)
GAIL P. ANDERSON
Contract Manager

Robert O'Neil
(Signature)
ROBERT O'NEIL
Branch Chief

FOR THE COMMANDER

R. Earl Good
(Signature)
R. EARL GOOD
Division Director
Optical/Infrared Technology Division

This report has been reviewed by the ESD Public Affairs Office (PA) and is releasable to the National Technical Information Service (NTIS).

Qualified requestors may obtain additional copies from the Defense Technical Information Center. All others should apply to the National Technical Information Service.

If your address has changed, or if you wish to be removed from the mailing list, or if the addressee is no longer employed by your organization, please notify AFGL/DAA, Hanscom AFB, MA 01731. This will assist us in maintaining a current mailing list.

Do not return copies of this report unless contractual obligations or notices on a specific document requires that it be returned.

Unclassified

SECURITY CLASSIFICATION OF THIS PAGE

REPORT DOCUMENTATION PAGE

1a. REPORT SECURITY CLASSIFICATION Unclassified			1b. RESTRICTIVE MARKINGS		
2a. SECURITY CLASSIFICATION AUTHORITY			3. DISTRIBUTION / AVAILABILITY OF REPORT Approved for public release; Distribution unlimited		
2b. DECLASSIFICATION / DOWNGRADING SCHEDULE			4. PERFORMING ORGANIZATION REPORT NUMBER(S)		
4. PERFORMING ORGANIZATION REPORT NUMBER(S)			5. MONITORING ORGANIZATION REPORT NUMBER(S) AFGL-TR-88-0161		
6a. NAME OF PERFORMING ORGANIZATION Smithsonian Institution		6b. OFFICE SYMBOL (if applicable)	7a. NAME OF MONITORING ORGANIZATION Air Force Geophysics Laboratory		
6c. ADDRESS (City, State, and ZIP Code) Astrophysical Observatory Cambridge, MA 02138			7b. ADDRESS (City, State, and ZIP Code) Hanscom AFB Massachusetts 01731-5000		
8a. NAME OF FUNDING / SPONSORING ORGANIZATION		8b. OFFICE SYMBOL (if applicable)	9. PROCUREMENT INSTRUMENT IDENTIFICATION NUMBER F19628-85-K-0049		
8c. ADDRESS (City, State, and ZIP Code)			10. SOURCE OF FUNDING NUMBERS		
		PROGRAM ELEMENT NO 62101F	PROJECT NO 7670	TASK NO 09	WORK UNIT ACCESSION NO AX
11. TITLE (Include Security Classification) Absolute Absorption Cross Section Measurements of Ozone and the Temperature Dependence at Four Reference Wavelengths Leading to Renormalization of the Cross Section Between 240 and 350 nm					
12. PERSONAL AUTHOR(S) W. H. Parkinson, K. Yoshino, D. E. Freeman					
13a. TYPE OF REPORT FINAL REPORT		13b. TIME COVERED FROM 7/24/85 TO 12/31/87	14. DATE OF REPORT (Year, Month, Day) 1988 March		15. PAGE COUNT 36
16. SUPPLEMENTARY NOTATION					
17. COSATI CODES			18. SUBJECT TERMS (Continue on reverse if necessary and identify by block number)		
FIELD	GROUP	SUB-GROUP	OZONE ABSORPTION CROSS SECTIONS; HARTLEY-HUGGINS BANDS; ULTRAVIOLET; TEMPERATURE DEPENDENCE; OPTICAL DEPTH.		
19. ABSTRACT (Continue on reverse if necessary and identify by block number) We have developed techniques for the preparation and preservation of pure ozone which have enabled its absolute cross section at an important mercury-line reference wavelength 253.7 nm and at iron line wavelengths 283.3, 245.8 and 263.7 nm to be determined at the temperatures 293, 228 and 195 K. Specially constructed absorption cells are used together with existing spectrometers and associated equipment and light sources which have already been employed successfully to study the absolute cross section of ozone at longer wavelengths. This determination of the temperature dependence of the absolute cross section at 238.3, 245.8, 253.7 and 263.7 nm permit renormalization of the full relative cross sections for ozone between 240 nm and 350 nm. A tabular and computer accessible form of the ozone cross sections data has been made at 5/cm intervals. These absolute cross sections and their temperature dependence are needed for accurate calculations of the atmospheric transmission in the visible and near ultraviolet regions.					
20. DISTRIBUTION / AVAILABILITY OF ABSTRACT <input checked="" type="checkbox"/> UNCLASSIFIED/UNLIMITED <input type="checkbox"/> SAME AS RPT <input type="checkbox"/> DTIC USERS			21. ABSTRACT SECURITY CLASSIFICATION Unclassified		
22a. NAME OF RESPONSIBLE INDIVIDUAL Gail Anderson			22b. TELEPHONE (Include Area Code) (617) 377-2335		22c. OFFICE SYMBOL AFGL/OPE

CONTENTS

1. Abstract of Objectives	1
2. Introduction	1
3. Absorption Cross Section Measurements of Ozone	3
3.1 Ozone Absorption Cell and Preparation of Ozone	3
3.2 Optical Depth Measurements	3
4. Results	4
5. Presentations	6
5.1 Publications	6
5.2 Presentation at Meetings and Seminars	6
Acknowledgement	7
References	9



Approved for	
W. J. ...	<input checked="" type="checkbox"/>
...	<input type="checkbox"/>
...	<input type="checkbox"/>
...	<input type="checkbox"/>
Distribution/	
Availability Codes	
...	
...	
...	
A-1	

1. Abstract of Objectives

We have developed techniques for the preparation and preservation of pure ozone which have enabled its absolute cross section at important mercury-line reference wavelength 253.7 nm and at iron line wavelengths 238.3, 245.8 and 263.7 nm to be determined at the temperatures 293, 228 and 195 K. Specially constructed absorption cells are used together with existing spectrometers and associated equipment and light sources which have already been employed successfully to study the absolute cross section of ozone at longer wavelengths. This determination of the temperature dependence of the absolute cross section at 238.3, 245.8, 253.7 and 263.7 nm permit renormalization of the full relative cross sections for ozone between 240 nm and 350 nm. A tabular and computer accessible form of the ozone cross sections data has been made at 5 cm⁻¹ intervals. These absolute cross sections and their temperature dependence are needed for accurate calculations of the atmospheric transmission in the visible and near ultraviolet regions.

2. Introduction

The atmospherically important molecule ozone occurs in the troposphere and stratosphere where the temperature ranges approximately from 200 K to 300 K. Accurate calculations of the atmospheric transmission in the visible and near ultraviolet regions therefore require laboratory values of the absorption cross section of ozone and its temperature dependence. In the usual method of determining the absorption cross section $\sigma(\lambda)$ of a molecule, the formula

$$\ln I_0(\lambda)/I(\lambda) = N\sigma(\lambda) \quad (1)$$

is used in which the measured quantities are the ratio of the incident flux

$I_0(\lambda)$ to that transmitted $I(\lambda)$ through the gas and the column density N of absorbing molecules. In the application to ozone the major difficulty has been that the ozone column density is generally not obtainable directly from measurements of the total pressure, because ozone is difficult to prepare free from oxygen and because it decomposes, especially under irradiation, into oxygen. However, we have found that, when special precautions are taken to prepare pure ozone and to prevent its subsequent decomposition, the column density can be obtained accurately from measurement of the total pressure, which can be used with measurements of the optical depth to yield accurate absorption cross sections of ozone.

In the present research, we have measured the absolute cross sections of ozone at 293 K, 228 K, and 195 K at the important mercury-line reference wavelength of 253.7 nm. Many cross section measurements of ozone have been made relative to the cross section at this wavelength. However, existing measurements of the absolute cross section at 253.7 nm are adequate only at room temperature and are unsatisfactory at lower temperatures. The determination of the temperature dependence of the absolute cross section at 253.7 nm would permit many relative cross section measurements in other wavelength region, such as of Bass and Paur (1981, 1985) and our own (Freeman et al., 1981), to be put on a firm absolute basis.

In addition to this investigation at 253.7 nm, which is the usually accepted reference wavelength, we have measured the cross sections of ozone and their temperature dependences at the wavelengths 238.28, 245.83 and 263.66 nm, at the same temperatures (293 K, 228 K and 195 K) at which the study at 253.7 nm is conducted. The results have been combined with the absolute cross sections of ozone at several discrete wavelengths in the region 289-335 nm made earlier. These results permit renormalization of

the full relative cross section of ozone between 240 and 350 nm. We have constructed a tabular computer-accessible array of ozone cross sections at intervals of 5 cm^{-1} .

3. Absorption Cross Section Measurements of Ozone

3.1 Ozone Absorption Cell and Preparation of Ozone

A specially designed ozone absorption cell, made primarily of Pyrex glass but possessing fused silica windows, has been constructed. The vacuum-tight cell has been out-gassed by baking under vacuum, and passivated by prolonged exposure to ozone. The entire ozone column is cooled to 228 K or 195 K by immersing the cell in stirred methanol which is cooled by a cold finger connected to an external refrigeration unit. The experimental arrangement is shown in Fig. 1. Tubes with silica windows at each end are mounted to the end of the absorption cell. The tubes are evacuated to prevent condensation of atmospheric water on the cooled windows and also to provide thermal insulation.

Ozone is prepared from pure oxygen (Airco grade 4.5 passed through a liquid nitrogen trap) at 78 K in a Tesla discharge, by cooling liquid ozone at 78 K, and purifying it by pumping off residual oxygen from the oxygen/ozone mixture at 78 K. The ozone was not stored on silica gel because it absorbs not only ozone but also oxygen.

3.2 Optical Depth Measurements

The background continuum is provided by a hydrogen discharge lamp that is connected to the entrance slit assembly of a 0.3 m Czerny-Turner monochromator. The hollow cathode or mercury lamp are set behind the

hydrogen discharge lamp and are used to locate the required wavelengths. A thermally controlled mercury lamp is also used as the background source at 253.7 nm. Slit heights are limited to 2 mm to cut down scattered light which is estimated to be about 2% with continuum radiation as the background source. At 253.7 nm, the mercury line is also used as background radiation in which case there is negligible scattered light.

The incident intensity (I_0) was measured after ozone in the absorption cell was pumped out through traps cooled with liquid nitrogen. Ozone trapped at liquid nitrogen temperature has a vapour pressure of 2.5 m Torr at 78 K (Hanson and Mauersberger, 1986) and was measured as 3 m Torr in our experiment. It should be noted that with 2.5 m Torr of ozone in the 10 cm cell about 1% absorption is expected at 253.7 nm where the cross section of ozone is $1.15 \times 10^{-17} \text{ cm}^2$. This significant absorption was taken into account when the incident intensity I_0 was measured.

4. Results

The absolute cross sections at the wavelengths 238.28, 245.83, 253.73 and 263.66 nm have been measured at 295 K, 228 K and 195 K. Those numbers are listed in Table 1 with the absolute cross sections measured previously for the longer wavelength region. All measurements except the one at 253.7 nm were obtained with the background continuum radiation from a hydrogen discharge or xenon arc. The optical depth, $\ln I_0/I$, has been limited to the range 2.0-0.5 in the entire set of measurements. The 0.7% uncertainty in the cross sections arises from the statistical scatter of 0.3-0.5% in the optical depths, uncertainty of 0.2% in the optical path length, uncertainties of 0.1-0.4% in the temperatures, and an uncertainty of 0.5% in the pressure measurement. Another possible source of error is the

purity of ozone which we assumed to be 100% pure to obtain the column density.

The absorption cross section of ozone at five mercury wavelengths are compared with those of previous work in Table 2, where only photoelectric measurements are collected. The agreement is reasonable at most wavelengths. All measurements are scattered within 2.5% of the average values but the values by Molina and Molina (1986) are slightly higher than other measurements, though by less than 1%. Without the values of Molina and Molina, all would agree within 1.5%. It should be emphasized that it is very difficult to achieve better than 1% uncertainty in photoabsorption cross section measurements and an additional problem is presented in the case of ozone because of its tendency to decompose. This agreement with many different techniques is quite satisfactory.

The values of the absolute cross sections of ozone at 195 K are compared with those from our published relative cross section measurements throughout the region 238-344 nm (Freeman *et al.*, 1984). The ratio of the absolute to the published numbers are listed in the sixth column of Table 1 of Quarterly Status Report No. 9. The cubic least-squares fit to those ratio leads to the smooth conversion factors for every wavelength and the conversion factors put our published numbers on an absolute bases. The results are shown in Table 3 at intervals of 5 cm^{-1} throughout the region of measurements and also are plotted in Fig. 2. In the same table, the calculated cross sections at 195 K from the parameters supplied by Bass are listed and their ratios are also listed in the same table. The calculated cross sections at 195 K by Bass are also plotted in Fig. 3. Except for the very longer wavelengths, both sets of numbers agree within 2-3%. In the longer wavelengths where band structures appear,

differences increase to around 20%, especially at the minimum absorption of the bands. We believe that the differences in the longer wavelengths are due to the limited sensitivity of Bass's technique for such weak absorption.

5. Presentations

5.1 Publications

Absolute Absorption Cross Section Measurements of Ozone in the Wavelength Region 238-335 nm and the Temperature Dependence, K. Yoshino, D.E. Freeman, J.R. Esmond, and W.H. Parkinson, Planet. Space Sci., accepted for publication.

5.2 Presentation at Meetings and Seminars

- 3/25/87 Seminar at Dalhousie University, Halifax, Canada.
High Resolution Ultraviolet Absorption Cross Sections of Atmospheric Molecules.
K. Yoshino
- 5/18-20/87 The Cambridge Meeting of the American Physical Society
The 18th Annual Meeting of the Division of Atomic, Molecular, and Optical Physics
High Resolution Absorption Cross Sections of Atmospheric Molecules in the Wavelength Region 175-350 nm
K. Yoshino, D.E. Freeman, A.S.-C. Cheung, J.R. Esmond and W.H. Parkinson

- 6/2-4/87 The 10th Annual Review Conference, AFGL, Bedford, MA
 Absolute Absorption Cross Section Measurements of Ozone and the
 Temperature Dependence
 K. Yoshino, D.E. Freeman, and W.H. Parkinson
- 6/15-19/87 42nd Symposium on Molecular Spectroscopy
 Absolute Absorption Cross Section Measurements of Ozone and
 the Temperature Dependence.
 K. Yoshino, D.E. Freeman, and W.H. Parkinson
- 10/27/87 Seminar at Herzberg Institute of Astrophysics, NRC, Canada
 High-Resolution VUV Studies of the Atmospheric Transmittance
 K. Yoshino

Acknowledgement

A part of this work was also supported by the NASA Upper Atmospheric Research Program under Grant No. NAG 5-144 to Harvard College Observatory. We thank Drs. Al Hall and G. Anderson of AFGL for their support for this work and for supplying parameters for temperature dependence of Bass's cross sections.

References

- Barnes, J. and Mauersberger, K. (1988) Temperature dependence of the ozone absorption cross section at the 253.7 nm mercury line, J. Geophys. Res., accepted for publication.
- Bass, A.M. and Paur, R.J. (1981) UV absorption cross sections for ozone: temperature dependence, J. Photochem. 17, 141.
- Bass, A.M. and Paur, R.J. (1985) The ultraviolet cross-sections of ozone: I. Measurements, in Atmospheric Ozone, Proceedings of the Quadrennial Ozone Symposium in Halkidiki, Greece, edited by C. Zeferos and A. Ghazi, pp. 606-616, D. Reidel, (Kluwer Academic Publishers, Hingham MA).
- Freeman, D.E., Yoshino, K., Esmond, J.R. and Parkinson, W.H. (1984) High resolution absorption cross-section measurements of ozone at 195 K in the wavelength region 240-350 nm, Planet. Space Sci. 32, 239.
- Hanson, D. and Mauersberger, K. (1986) The vapor pressures of solid and liquid ozone, J. Chem. Phys. 85, 4669.
- Malicet, J., Brion, J. and Daumont, D. (1985) New values of ozone absolute cross-sections in the ultraviolet spectral range at 298 and 228 K, by Method Based upon Pressure Measurements at Constant Volume, in Atmospheric Ozone, Proceedings of the Quadrennial Ozone Symposium in Halkidiki, Greece, edited by C. Zeferos and A. Ghazi, pp. 617-621, (Kluwer Academic Publishers, Hingham MA).
- Mauersberger, K., Barnes, J., Hanson, D. and Morton, J. (1986) Measurements of the ozone absorption cross-section at the 253.7 nm mercury line, Geophys. Res. Lett. 13, 671.
- Hearn, A.G. (1961) The absorption of ozone in the ultra-violet and visible regions of the spectrum, Proc. Phys. Soc. 78, 932.
- Inn, E.C.Y. and Tanaka, Y. (1953) Absorption coefficients of ozone in the

ultraviolet and visible region, J. Opt. Soc. Am. 43, 870.

Molina, L.T. and Molina, M.J. (1986) Absolute absorption cross sections of ozone in the 185-350 nm wavelength range, J. Geophys. Res. 91, 14501.

Table 1. Absorption Cross Sections of Ozone, in Units of 10^{-x} cm^2

Wavelength (nm)		x	Cross Sections ^a		
Vacuum	Air		295 K	228 K	195 K
238.2762	238.2035	18	7.45 [15]	7.51 [15]	7.51 [52]
245.8341	245.7597	17	1.010 [9]	1.006 [11]	1.017 [9]
253.7279	253.6517	17	1.144 [8]	1.154 [10]	1.152 [10]
253.7279	253.6517 (Hg)	17	1.145 [26]	1.155 [18]	1.151 [15]
263.6594	263.5809	18	9.71 [9]	9.66 [9]	9.64 [11]
272.1708	272.0902	18	6.82 [4]	6.70 [4]	6.67 [2]
281.4115	281.3286	18	3.52 [6]	3.31 [4]	3.30 [5]
289.4446 ^b	289.3598	18	1.488 [5]	1.402 [4]	1.399 [5]
296.8150 ^b	296.7284	19	5.97 [6]	5.60 [4]	5.50 [5]
302.2380 ^b	302.1500	19	2.91 [5]	2.65 [5]	2.58 [5]
314.2242	314.1332	20	5.86 [5]	4.86 [5]	4.80 [5]
322.1649	322.0719	20	2.39 [6]	2.15 [4]	2.20 [3]
334.2442 ^b	334.1481	21	4.37 [3]	3.11 [3]	2.93 [3]
344.3526	344.2539	21	1.132 [3]	0.974 [3]	0.843 [3]

^aThe numbers in the brackets are the numbers of optical depth measurements.

^bCross sections were presented previously [Freeman et al., 1985].

Table 2. Absorption Cross Sections of Ozone in Units of 10^{-x} cm²,
at Hg I Wavelengths

	Temperature K	x=17	18	19	19	21
		Cross Section				
		λ 253.6	λ 289.3	λ 296.7	λ 302.1	λ 334.1
YFEP ^a (1988)	295	1.145	1.488	5.97	2.91	4.37
	228	1.155	1.402	5.60	2.65	3.11
MM ^b (1986)	298	1.157	1.540	6.229	3.027	4.46
	226	1.166	1.468	5.766	2.720	3.22
MBHM ^c (1986)	297	1.137				
BM ^d (1987)	297	1.136				
	221	1.144				
BP ^e (1985)	298		1.501	6.07	2.94	4.7
	228		1.423	5.59	2.64	3.5
MBD ^f (1985)	298		1.436	5.83	2.83	4.28
H ^g (1961)	294	1.147	1.47	5.971	2.860	4.27
IT ^h (1953)	295	1.140	1.46	5.76	2.84	5.22

^aYoshino, Freeman, Esmond and Parkinson, present work

^bMolina and Molina (1986)

^cMauersberger, Barnes, Hanson and Morton (1986)

^dBarnes and Mauersberger (1987)

^eBass and Paur (1985)

^fMalicet, Brion and Daumont (1985)

^gHearn (1961)

^hInn and Tanaka (1953)

Table 3

Comparison of ozone cross sections at 195 K: HCO and Bass data with RATIO - Bass / HCO

(1)

Wavenumber	HCO	BASS	RATIO	Wavenumber	HCO	BASS	RATIO	Wavenumber	HCO	BASS	RATIO
28600.000	3.21E-23			28875.000	9.90E-23			29150.000	2.26E-22	5.12E-22	2.266
28605.000	3.10E-23			28880.000	1.01E-22			29155.000	2.01E-22	5.14E-22	2.558
28610.000	2.65E-23			28885.000	1.05E-22			29160.000	1.94E-22	4.90E-22	2.524
28615.000	2.62E-23			28890.000	1.09E-22			29165.000	1.77E-22	4.65E-22	2.628
28620.000	3.01E-23			28895.000	1.24E-22			29170.000	1.63E-22	4.41E-22	2.704
28625.000	3.29E-23			28900.000	1.27E-22			29175.000	1.54E-22	4.16E-22	2.703
28630.000	3.08E-23			28905.000	1.37E-22			29180.000	1.58E-22	3.92E-22	2.479
28635.000	3.47E-23			28910.000	1.47E-22			29185.000	1.55E-22	3.67E-22	2.369
28640.000	3.47E-23			28915.000	1.51E-22			29190.000	1.51E-22	3.52E-22	2.334
28645.000	3.76E-23			28920.000	1.54E-22			29195.000	1.61E-22	3.61E-22	2.244
28650.000	3.58E-23			28925.000	1.61E-22			29200.000	1.69E-22	3.70E-22	2.191
28655.000	4.17E-23			28930.000	1.66E-22			29205.000	1.69E-22	3.79E-22	2.244
28660.000	3.98E-23			28935.000	1.65E-22			29210.000	1.77E-22	3.88E-22	2.193
28665.000	4.46E-23			28940.000	1.67E-22			29215.000	1.81E-22	3.97E-22	2.194
28670.000	4.75E-23			28945.000	1.79E-22			29220.000	1.96E-22	4.06E-22	2.071
28675.000	5.95E-23			28950.000	1.95E-22			29225.000	2.00E-22	4.15E-22	2.074
28680.000	5.53E-23			28955.000	2.13E-22			29230.000	2.13E-22	4.24E-22	1.990
28685.000	5.53E-23			28960.000	2.24E-22			29235.000	2.11E-22	4.20E-22	1.990
28690.000	6.21E-23			28965.000	2.38E-22			29240.000	2.20E-22	4.32E-22	1.871
28695.000	6.67E-23			28970.000	2.56E-22			29245.000	2.21E-22	4.04E-22	1.826
28700.000	6.27E-23			28975.000	2.67E-22			29250.000	2.29E-22	3.95E-22	1.727
28705.000	7.16E-23			28980.000	2.99E-22			29255.000	2.35E-22	3.87E-22	1.648
28710.000	7.71E-23			28985.000	3.19E-22			29260.000	2.49E-22	3.79E-22	1.523
28715.000	9.02E-23			28990.000	3.56E-22			29265.000	2.50E-22	3.71E-22	1.484
28720.000	8.88E-23			28995.000	3.75E-22			29270.000	2.69E-22	4.02E-22	1.494
28725.000	1.07E-22			29000.000	4.08E-22			29275.000	2.75E-22	4.36E-22	1.586
28730.000	1.15E-22			29005.000	4.68E-22			29280.000	2.93E-22	4.71E-22	1.606
28735.000	1.24E-22			29010.000	4.97E-22			29285.000	3.23E-22	5.05E-22	1.563
28740.000	1.33E-22			29015.000	5.33E-22			29290.000	3.39E-22	5.39E-22	1.591
28745.000	1.42E-22			29020.000	5.96E-22			29295.000	3.81E-22	5.74E-22	1.506
28750.000	1.60E-22			29025.000	6.53E-22			29300.000	3.96E-22	6.08E-22	1.535
28755.000	1.82E-22			29030.000	7.10E-22			29305.000	4.32E-22	6.42E-22	1.487
28760.000	1.94E-22			29035.000	7.79E-22			29310.000	4.71E-22	6.77E-22	1.437
28765.000	2.06E-22			29040.000	8.40E-22			29315.000	5.09E-22	7.11E-22	1.397
28770.000	2.38E-22			29045.000	9.08E-22			29320.000	5.62E-22	7.46E-22	1.327
28775.000	2.49E-22			29050.000	9.71E-22			29325.000	6.02E-22	7.80E-22	1.296
28780.000	2.61E-22			29055.000	1.04E-21			29330.000	6.56E-22	8.14E-22	1.241
28785.000	2.76E-22			29060.000	1.09E-21			29335.000	6.99E-22	8.49E-22	1.214
28790.000	2.91E-22			29065.000	1.11E-21			29340.000	7.76E-22	8.83E-22	1.138
28795.000	3.01E-22			29070.000	1.08E-21			29345.000	8.50E-22	9.17E-22	1.079
28800.000	2.91E-22			29075.000	9.60E-22			29350.000	9.31E-22	9.52E-22	1.022
28805.000	2.35E-22			29080.000	7.19E-22			29355.000	1.03E-21	9.86E-22	0.957
28810.000	1.53E-22			29085.000	5.21E-22			29360.000	1.11E-21	1.02E-21	0.919
28815.000	1.11E-22			29090.000	4.26E-22			29365.000	1.23E-21	1.06E-21	0.858
28820.000	8.22E-23			29095.000	3.88E-22			29370.000	1.31E-21	1.09E-21	0.832
28825.000	6.53E-23			29100.000	3.67E-22			29375.000	1.42E-21	1.12E-21	0.791
28830.000	6.44E-23			29105.000	3.50E-22			29380.000	1.54E-21	1.16E-21	0.752
28835.000	6.44E-23			29110.000	3.53E-22			29385.000	1.61E-21	1.19E-21	0.741
28840.000	6.44E-23			29115.000	3.58E-22			29390.000	1.66E-21	1.23E-21	0.739
28845.000	6.22E-23			29120.000	3.66E-22			29395.000	1.68E-21	1.26E-21	0.751
28850.000	7.12E-23			29125.000	3.70E-22			29400.000	1.60E-21	1.23E-21	0.768
28855.000	7.97E-23			29130.000	3.76E-22			29405.000	1.36E-21	1.14E-21	0.836
28860.000	8.75E-23			29135.000	3.62E-22			29410.000	1.02E-21	8.64E-22	0.847
28865.000	8.23E-23			29140.000	3.19E-22			29415.000	7.73E-22	6.87E-22	0.889
28870.000	9.34E-23			29145.000	2.70E-22			29420.000	6.57E-22	6.65E-22	1.014

Comparison of ozone cross sections at 195 K: HCO and Bass data with RATIO = Bass / HCO (8)

Wavenumber	HCO	BASS	RATIO	Wavenumber	HCO	BASS	RATIO	Wavenumber	HCO	BASS	RATIO
34375.000	1.18E-18	1.20E-18	1.019	34650.000	1.54E-18	1.54E-18	1.001	34925.000	2.05E-18	2.06E-18	1.005
34380.000	1.20E-18	1.21E-18	1.008	34655.000	1.54E-18	1.56E-18	1.011	34930.000	2.05E-18	2.06E-18	1.007
34385.000	1.21E-18	1.21E-18	1.003	34660.000	1.55E-18	1.56E-18	1.009	34935.000	2.06E-18	2.07E-18	1.008
34390.000	1.22E-18	1.22E-18	0.996	34665.000	1.56E-18	1.57E-18	1.004	34940.000	2.08E-18	2.10E-18	1.008
34395.000	1.22E-18	1.23E-18	1.007	34670.000	1.57E-18	1.57E-18	1.001	34945.000	2.08E-18	2.11E-18	1.013
34400.000	1.23E-18	1.23E-18	1.006	34675.000	1.56E-18	1.57E-18	1.006	34950.000	2.11E-18	2.12E-18	1.003
34405.000	1.23E-18	1.24E-18	1.008	34680.000	1.57E-18	1.58E-18	1.004	34955.000	2.09E-18	2.13E-18	1.019
34410.000	1.22E-18	1.24E-18	1.019	34685.000	1.58E-18	1.58E-18	1.001	34960.000	2.12E-18	2.15E-18	1.013
34415.000	1.22E-18	1.24E-18	1.020	34690.000	1.58E-18	1.59E-18	1.005	34965.000	2.13E-18	2.14E-18	1.005
34420.000	1.25E-18	1.25E-18	1.000	34695.000	1.58E-18	1.59E-18	0.009	34970.000	2.14E-18	2.15E-18	1.003
34425.000	1.25E-18	1.26E-18	1.007	34700.000	1.60E-18	1.60E-18	1.001	34975.000	2.14E-18	2.16E-18	1.008
34430.000	1.25E-18	1.26E-18	1.012	34705.000	1.61E-18	1.60E-18	0.997	34980.000	2.15E-18	2.17E-18	1.007
34435.000	1.26E-18	1.27E-18	1.010	34710.000	1.62E-18	1.61E-18	0.993	34985.000	2.14E-18	2.16E-18	1.012
34440.000	1.26E-18	1.27E-18	1.011	34715.000	1.63E-18	1.63E-18	0.999	34990.000	2.15E-18	2.17E-18	1.010
34445.000	1.26E-18	1.28E-18	1.014	34720.000	1.62E-18	1.64E-18	1.011	34995.000	2.14E-18	2.17E-18	1.015
34450.000	1.27E-18	1.28E-18	1.011	34725.000	1.64E-18	1.64E-18	1.004	35000.000	2.13E-18	2.17E-18	1.018
34455.000	1.27E-18	1.29E-18	1.014	34730.000	1.65E-18	1.66E-18	1.004	35005.000	2.14E-18	2.16E-18	1.012
34460.000	1.29E-18	1.30E-18	1.006	34735.000	1.66E-18	1.67E-18	1.005	35010.000	2.13E-18	2.17E-18	1.017
34465.000	1.29E-18	1.30E-18	1.011	34740.000	1.67E-18	1.68E-18	1.008	35015.000	2.13E-18	2.17E-18	1.019
34470.000	1.29E-18	1.31E-18	1.017	34745.000	1.68E-18	1.68E-18	1.004	35020.000	2.14E-18	2.17E-18	1.016
34475.000	1.30E-18	1.31E-18	1.009	34750.000	1.70E-18	1.70E-18	0.999	35025.000	2.14E-18	2.18E-18	1.019
34480.000	1.30E-18	1.32E-18	1.013	34755.000	1.72E-18	1.72E-18	0.998	35030.000	2.17E-18	2.19E-18	1.008
34485.000	1.31E-18	1.32E-18	1.009	34760.000	1.74E-18	1.73E-18	0.997	35035.000	2.16E-18	2.20E-18	1.017
34490.000	1.31E-18	1.32E-18	1.008	34765.000	1.74E-18	1.75E-18	1.005	35040.000	2.16E-18	2.21E-18	1.025
34495.000	1.31E-18	1.33E-18	1.013	34770.000	1.76E-18	1.77E-18	1.005	35045.000	2.20E-18	2.22E-18	1.009
34500.000	1.32E-18	1.33E-18	1.006	34775.000	1.78E-18	1.78E-18	1.002	35050.000	2.22E-18	2.24E-18	1.007
34505.000	1.32E-18	1.33E-18	1.009	34780.000	1.81E-18	1.80E-18	0.994	35055.000	2.23E-18	2.25E-18	1.010
34510.000	1.33E-18	1.34E-18	1.007	34785.000	1.82E-18	1.82E-18	0.999	35060.000	2.25E-18	2.27E-18	1.011
34515.000	1.34E-18	1.35E-18	1.008	34790.000	1.84E-18	1.84E-18	1.000	35065.000	2.26E-18	2.30E-18	1.016
34520.000	1.35E-18	1.36E-18	1.008	34795.000	1.84E-18	1.85E-18	1.006	35070.000	2.29E-18	2.31E-18	1.007
34525.000	1.35E-18	1.37E-18	1.012	34800.000	1.85E-18	1.86E-18	1.005	35075.000	2.30E-18	2.32E-18	1.008
34530.000	1.36E-18	1.37E-18	1.008	34805.000	1.87E-18	1.87E-18	1.001	35080.000	2.31E-18	2.33E-18	1.007
34535.000	1.38E-18	1.38E-18	1.000	34810.000	1.86E-18	1.88E-18	1.012	35085.000	2.35E-18	2.33E-18	0.993
34540.000	1.38E-18	1.39E-18	1.010	34815.000	1.88E-18	1.89E-18	1.005	35090.000	2.35E-18	2.35E-18	0.998
34545.000	1.39E-18	1.40E-18	1.007	34820.000	1.88E-18	1.89E-18	1.007	35095.000	2.37E-18	2.37E-18	1.006
34550.000	1.40E-18	1.40E-18	0.997	34825.000	1.90E-18	1.89E-18	0.996	35100.000	2.36E-18	2.39E-18	1.003
34555.000	1.40E-18	1.42E-18	1.013	34830.000	1.89E-18	1.91E-18	1.009	35105.000	2.38E-18	2.40E-18	0.998
34560.000	1.42E-18	1.43E-18	1.008	34835.000	1.90E-18	1.92E-18	1.008	35110.000	2.40E-18	2.40E-18	0.996
34565.000	1.43E-18	1.43E-18	1.001	34840.000	1.92E-18	1.91E-18	0.997	35115.000	2.41E-18	2.41E-18	0.998
34570.000	1.43E-18	1.44E-18	1.004	34845.000	1.91E-18	1.91E-18	1.000	35120.000	2.41E-18	2.41E-18	0.998
34575.000	1.43E-18	1.44E-18	1.010	34850.000	1.92E-18	1.92E-18	0.998	35125.000	2.41E-18	2.41E-18	0.999
34580.000	1.44E-18	1.45E-18	1.009	34855.000	1.90E-18	1.92E-18	1.013	35130.000	2.41E-18	2.42E-18	1.004
34585.000	1.45E-18	1.47E-18	1.013	34860.000	1.92E-18	1.93E-18	1.005	35135.000	2.42E-18	2.43E-18	1.003
34590.000	1.45E-18	1.47E-18	1.011	34865.000	1.93E-18	1.93E-18	1.001	35140.000	2.45E-18	2.43E-18	0.993
34595.000	1.46E-18	1.46E-18	1.003	34870.000	1.93E-18	1.93E-18	1.002	35145.000	2.46E-18	2.45E-18	0.995
34600.000	1.47E-18	1.47E-18	1.003	34875.000	1.94E-18	1.93E-18	1.004	35150.000	2.46E-18	2.46E-18	0.998
34605.000	1.47E-18	1.49E-18	1.004	34880.000	1.95E-18	1.95E-18	1.001	35155.000	2.46E-18	2.46E-18	1.002
34610.000	1.49E-18	1.49E-18	1.002	34885.000	1.96E-18	1.97E-18	1.003	35160.000	2.46E-18	2.47E-18	1.005
34615.000	1.50E-18	1.50E-18	1.003	34890.000	1.98E-18	1.98E-18	0.996	35165.000	2.46E-18	2.48E-18	1.006
34620.000	1.50E-18	1.50E-18	1.003	34895.000	1.98E-18	1.98E-18	1.007	35170.000	2.46E-18	2.47E-18	1.006
34625.000	1.51E-18	1.51E-18	1.002	34900.000	2.00E-18	2.00E-18	1.002	35175.000	2.46E-18	2.47E-18	1.002
34630.000	1.51E-18	1.52E-18	1.007	34905.000	2.01E-18	2.01E-18	1.002	35180.000	2.49E-18	2.48E-18	0.998
34635.000	1.51E-18	1.53E-18	1.012	34910.000	2.02E-18	2.03E-18	1.004	35185.000	2.48E-18	2.49E-18	1.003
34640.000	1.52E-18	1.54E-18	1.012	34915.000	2.03E-18	2.04E-18	1.006	35190.000	2.51E-18	2.49E-18	0.992
34645.000	1.53E-18	1.54E-18	1.004	34920.000	2.03E-18	2.05E-18	1.012	35195.000	2.53E-18	2.50E-18	0.987

Comparison of ozone cross sections at 195 K: HCO and Bass data with RATIO = Bass / HCO (16)

Wavenumber	HCO	BASS	RATIO	Wavenumber	HCO	BASS	RATIO	Wavenumber	HCO	BASS	RATIO
40975.000	9.58E-18			41250.000	8.96E-18			41525.000	8.39E-18		
40980.000	9.57E-18			41255.000	8.95E-18			41530.000	8.41E-18		
40985.000	9.59E-18			41260.000	8.91E-18			41535.000	8.34E-18		
40990.000	9.57E-18			41265.000	8.92E-18			41540.000	8.32E-18		
40995.000	9.48E-18			41270.000	8.91E-18			41545.000	8.26E-18		
41000.000	9.47E-18	9.72E-18	1.026	41275.000	8.87E-18			41550.000	8.32E-18		
41005.000	9.55E-18			41280.000	8.96E-18			41555.000	8.29E-18		
41010.000	9.55E-18			41285.000	8.95E-18			41560.000	8.24E-18		
41015.000	9.61E-18			41290.000	9.01E-18			41565.000	8.22E-18		
41020.000	9.54E-18			41295.000	9.01E-18			41570.000	8.26E-18		
41025.000	9.53E-18			41300.000	8.97E-18	9.02E-18	1.006	41575.000	8.18E-18		
41030.000	9.53E-18			41305.000	8.93E-18			41580.000	8.23E-18		
41035.000	9.50E-18			41310.000	8.85E-18			41585.000	8.25E-18		
41040.000	9.48E-18			41315.000	8.77E-18			41590.000	8.22E-18		
41045.000	9.38E-18			41320.000	8.85E-18			41595.000	8.21E-18		
41050.000	9.38E-18			41325.000	8.81E-18			41600.000	8.17E-18	8.39E-18	1.027
41055.000	9.41E-18			41330.000	8.81E-18			41605.000	8.14E-18		
41060.000	9.46E-18			41335.000	8.85E-18			41610.000	8.11E-18		
41065.000	9.42E-18			41340.000	8.86E-18			41615.000	8.16E-18		
41070.000	9.43E-18			41345.000	8.88E-18			41620.000	8.25E-18		
41075.000	9.44E-18			41350.000	8.86E-18			41625.000	8.23E-18		
41080.000	9.32E-18			41355.000	8.81E-18			41630.000	8.18E-18		
41085.000	9.41E-18			41360.000	8.74E-18			41635.000	8.15E-18		
41090.000	9.43E-18			41365.000	8.85E-18			41640.000	8.16E-18		
41095.000	9.44E-18			41370.000	8.78E-18			41645.000	8.17E-18		
41100.000	9.32E-18	9.51E-18	1.020	41375.000	8.78E-18			41650.000	8.17E-18		
41105.000	9.32E-18			41380.000	8.71E-18			41655.000	8.23E-18		
41110.000	9.34E-18			41385.000	8.70E-18			41660.000	8.19E-18		
41115.000	9.28E-18			41390.000	8.75E-18			41665.000	8.19E-18		
41120.000	9.21E-18			41395.000	8.68E-18			41670.000	8.17E-18		
41125.000	9.27E-18			41400.000	8.69E-18	8.91E-18	1.025	41675.000	8.15E-18		
41130.000	9.27E-18			41405.000	8.68E-18			41680.000	8.18E-18		
41135.000	9.25E-18			41410.000	8.63E-18			41685.000	8.08E-18		
41140.000	9.24E-18			41415.000	8.61E-18			41690.000	8.13E-18		
41145.000	9.22E-18			41420.000	8.59E-18			41695.000	8.13E-18		
41150.000	9.20E-18			41425.000	8.62E-18			41700.000	8.14E-18	8.28E-18	1.017
41155.000	9.19E-18			41430.000	8.62E-18			41705.000	8.16E-18		
41160.000	9.22E-18			41435.000	8.58E-18			41710.000	8.06E-18		
41165.000	9.18E-18			41440.000	8.60E-18			41715.000	8.08E-18		
41170.000	9.14E-18			41445.000	8.56E-18			41720.000	8.09E-18		
41175.000	9.07E-18			41450.000	8.48E-18			41725.000	8.00E-18		
41180.000	9.08E-18			41455.000	8.49E-18			41730.000	7.95E-18		
41185.000	9.14E-18			41460.000	8.53E-18			41735.000	7.96E-18		
41190.000	9.16E-18			41465.000	8.58E-18			41740.000	8.00E-18		
41195.000	9.04E-18			41470.000	8.52E-18			41745.000	7.96E-18		
41200.000	9.03E-18	9.24E-18	1.023	41475.000	8.57E-18			41750.000	7.96E-18		
41205.000	9.05E-18			41480.000	8.45E-18			41755.000	7.95E-18		
41210.000	8.96E-18			41485.000	8.45E-18			41760.000	7.93E-18		
41215.000	9.02E-18			41490.000	8.44E-18			41765.000	7.91E-18		
41220.000	9.07E-18			41495.000	8.45E-18			41770.000	7.86E-18		
41225.000	8.98E-18			41500.000	8.41E-18	8.60E-18	1.023	41775.000	7.80E-18		
41230.000	8.98E-18			41505.000	8.39E-18			41780.000	7.83E-18		
41235.000	8.93E-18			41510.000	8.36E-18			41785.000	7.79E-18		
41240.000	8.97E-18			41515.000	8.32E-18			41790.000	7.81E-18		
41245.000	8.92E-18			41520.000	8.39E-18			41795.000	7.77E-18		

Comparison of ozone cross sections at 195 K: HCO and Bass data with RATIO = Bass / HCO

Wavenumber	HCO	BASS	RATIO	Wavenumber	HCO	BASS	RATIO
41800.000	7.71E-18	7.96E-18	1.032	42075.000	7.24E-18		
41805.000	7.70E-18			42080.000	7.25E-18		
41810.000	7.76E-18			42085.000	7.17E-18		
41815.000	7.80E-18			42090.000	7.07E-18		
41820.000	7.72E-18			42095.000	7.09E-18		
41825.000	7.65E-18			42100.000	7.09E-18	7.31E-18	1.031
41830.000	7.61E-18			42105.000	7.15E-18		
41835.000	7.67E-18			42110.000	7.18E-18		
41840.000	7.71E-18			42115.000	7.13E-18		
41845.000	7.68E-18			42120.000	7.08E-18		
41850.000	7.64E-18			42125.000	7.11E-18		
41855.000	7.64E-18			42130.000	7.11E-18		
41860.000	7.63E-18			42135.000	6.97E-18		
41865.000	7.61E-18			42140.000	7.03E-18		
41870.000	7.63E-18			42145.000	7.08E-18		
41875.000	7.60E-18			42150.000	7.06E-18		
41880.000	7.56E-18			42155.000	7.07E-18		
41885.000	7.67E-18			42160.000	7.02E-18		
41890.000	7.56E-18			42165.000	7.00E-18		
41895.000	7.59E-18			42170.000	7.07E-18		
41900.000	7.56E-18	7.74E-18	1.023	42175.000	7.04E-18		
41905.000	7.50E-18			42180.000	6.96E-18		
41910.000	7.48E-18			42185.000	6.98E-18		
41915.000	7.53E-18			42190.000	6.97E-18		
41920.000	7.48E-18			42195.000	7.03E-18		
41925.000	7.50E-18			42200.000	6.98E-18	7.10E-18	1.018
41930.000	7.49E-18			42205.000	6.93E-18		
41935.000	7.53E-18			42210.000	6.86E-18		
41940.000	7.47E-18			42215.000	6.93E-18		
41945.000	7.46E-18			42220.000	6.88E-18		
41950.000	7.47E-18			42225.000	6.91E-18		
41955.000	7.45E-18			42230.000	6.92E-18		
41960.000	7.40E-18			42235.000	6.81E-18		
41965.000	7.44E-18			42240.000	6.84E-18		
41970.000	7.56E-18			42245.000	6.86E-18		
41975.000	7.45E-18			42250.000	6.76E-18		
41980.000	7.39E-18			42255.000	6.73E-18		
41985.000	7.44E-18			42260.000	6.81E-18		
41990.000	7.36E-18			42265.000	6.76E-18		
41995.000	7.35E-18			42265.000	6.76E-18		
42000.000	7.33E-18	7.55E-18	1.030				
42005.000	7.31E-18						
42010.000	7.40E-18						
42015.000	7.34E-18						
42020.000	7.28E-18						
42025.000	7.24E-18						
42030.000	7.35E-18						
42035.000	7.32E-18						
42040.000	7.32E-18						
42045.000	7.33E-18						
42050.000	7.25E-18						
42055.000	7.21E-18						
42060.000	7.25E-18						
42065.000	7.20E-18						
42070.000	7.19E-18						

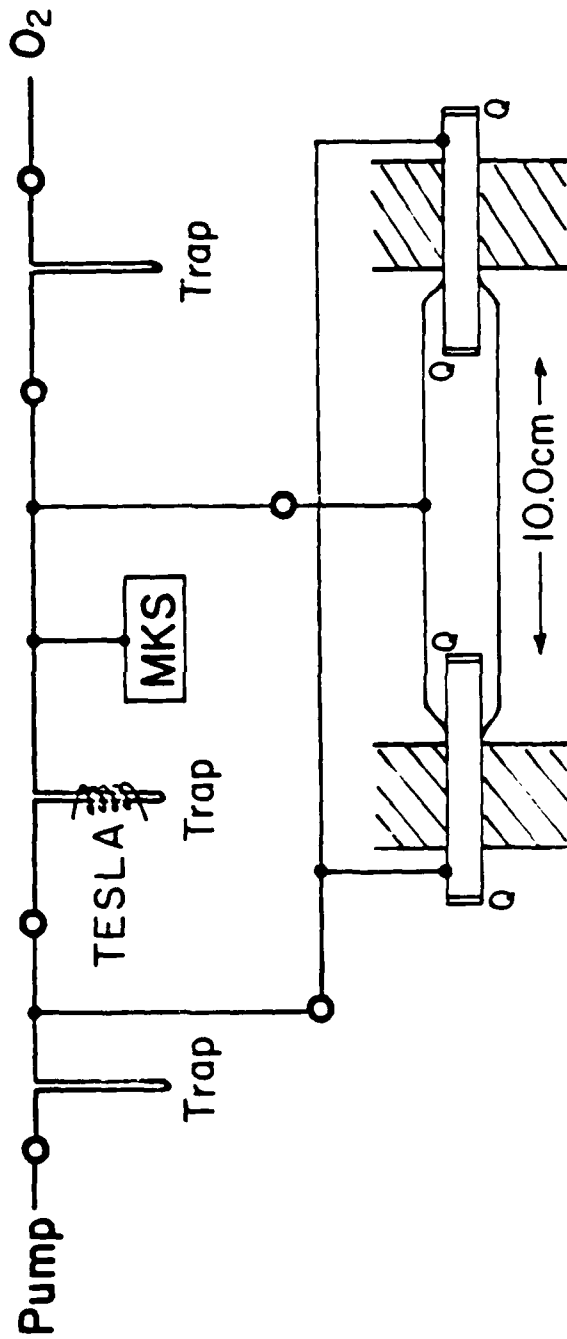


Figure 1. Experimental arrangement for preparation of ozone

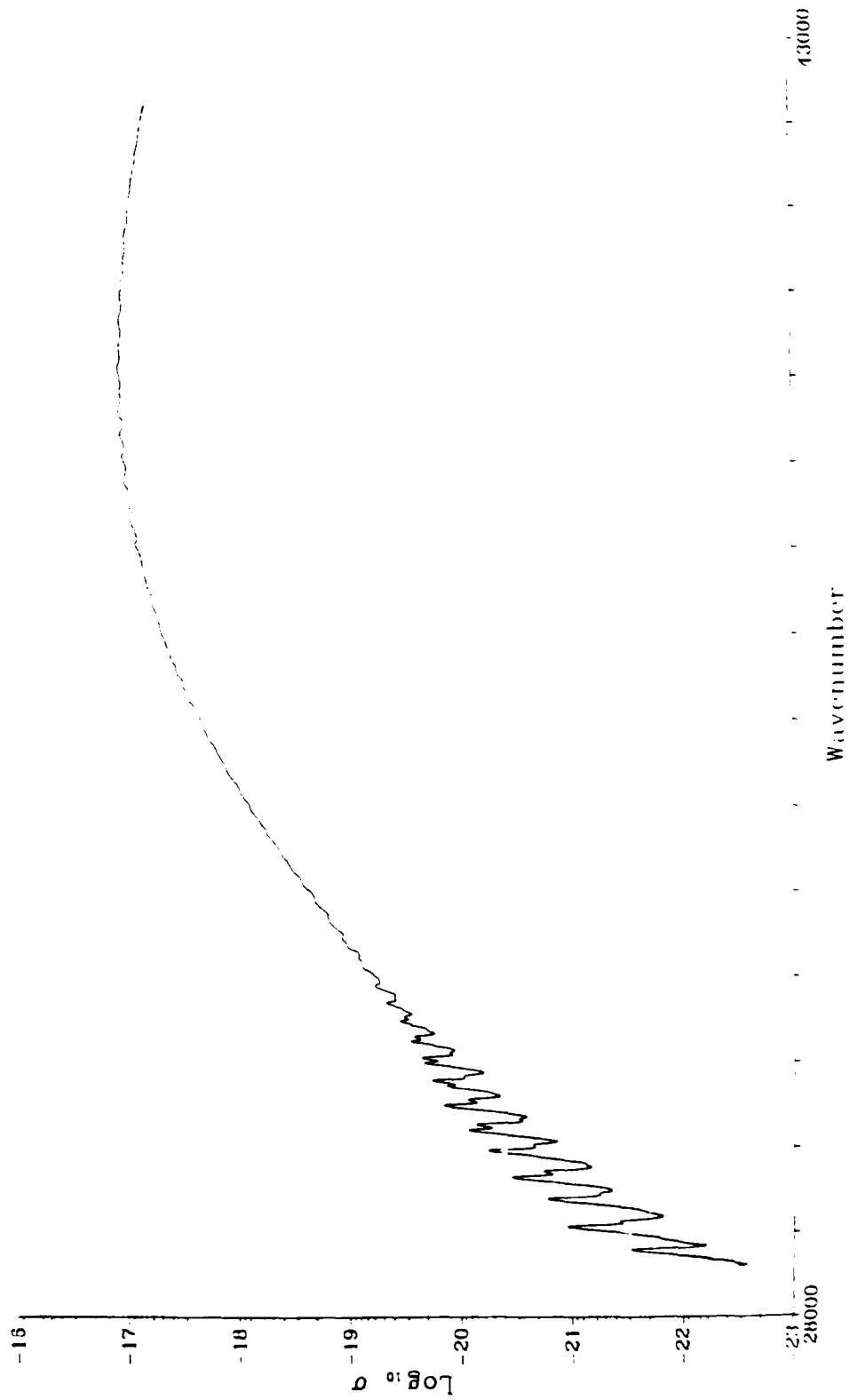


Figure 2. The cross sections of ozone at 195 K in the absolute base by the present measurements from our published relative measurements.

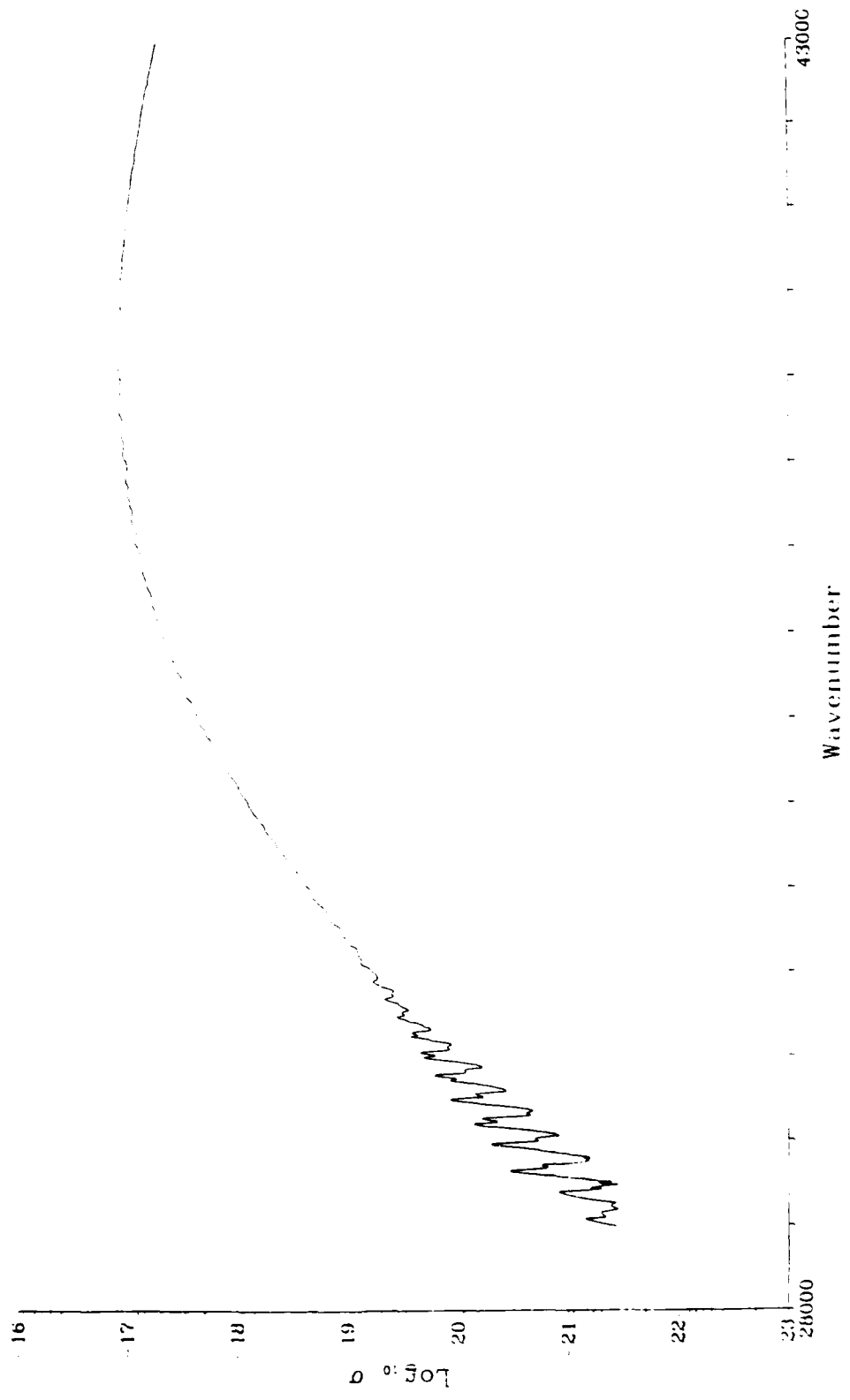


Figure 3. The cross sections of ozone at 195 K calculated from parameters supplied by Bass.